Since January 2020 Elsevier has created a COVID-19 resource centre with free information in English and Mandarin on the novel coronavirus COVID-19. The COVID-19 resource centre is hosted on Elsevier Connect, the company's public news and information website.

Elsevier hereby grants permission to make all its COVID-19-related research that is available on the COVID-19 resource centre - including this research content - immediately available in PubMed Central and other publicly funded repositories, such as the WHO COVID database with rights for unrestricted research re-use and analyses in any form or by any means with acknowledgement of the original source. These permissions are granted for free by Elsevier for as long as the COVID-19 resource centre remains active.

Current Problems in Diagnostic Radiology 51 (2022) 112–120

Current Problems in Diagnostic Radiology

journal homepage: www.cpdrjournal.com

Magnetic Resonance Imaging in Coronavirus Disease - 2019 Associated Rhino-Orbital-Cerebral Mucormycosis (CA-ROCM) - Imaging Analysis of 50 Consecutive Patients

Taruna Yadav, MD [a], Sarbesh Tiwari, MD, DM[a,*], Aanchal Gupta, MBBS[a], Pawan Kumar Garg, MD[a], Pushpinder Singh Khera, MD[a], Rengarajan Rajagopal, MD, DM[a], Amit Goyal, MS[b], Kapil Soni, MS[b], Ankita Chugh, BDS, MDS[c], Vidhi Jain, MD[d], Binit Sureka, MD[a], Poonam Elhence, MD[e], Sanjeev Misra, MS,MCh[f]

[a] *Department of Diagnostic and Interventional radiology, All India Institute of Medical Sciences, Jodhpur, Rajasthan, India*
[b] *Department of E.N.T.-Otorhinolaryngology, All India Institute of Medical Sciences, Jodhpur, Rajasthan, India*
[c] *Department of Dentistry, All India Institute of Medical Sciences, Jodhpur, Rajasthan, India*
[d] *Department of Microbiology, All India Institute of Medical Sciences, Jodhpur, Rajasthan, India*
[e] *Department of Pathology, All India Institute of Medical Sciences, Jodhpur, Rajasthan, India*
[f] *Professor Department of Surgical Oncology, Director and CEO, All India Institute of Medical Sciences, Jodhpur, Rajasthan, India*

A B S T R A C T

Background and Purpose: Rhino-orbital-cerebral mucormycosis has emerged as a major opportunistic infection in patients with COVID-19. High clinical suspicion and prompt imaging are crucial for early diagnosis and management. Our study evaluates imaging characteristics of patients with COVID-19 associated Rhino-orbital-cerebral Mucormycosis (CA-ROCM) in a tertiary care hospital in India.

Materials and Methods: A retrospective analysis of clinical and imaging data of patients with CA-ROCM who presented between December 2020 to June 2021 was performed. All patients had microbiologically or histologically proven sino-nasal mucormycosis along with documented SARS-CoV-2 positive RT-PCR test and/or classical lung imaging features of COVID-19 infection. The extent of sinus involvement, bony erosions, extra-sinus soft tissue extension, orbital-intracranial invasion, perineural spread, and vascular complications were assessed.

Results: Fifty patients were included for the final analysis. Diabetes was the most common associated comorbidity. Seven patients presented with stage I disease, 18 patients with stage II, and 25 patients with stage III disease. The stage of disease showed a positive statistical correlation with HbA1c levels using Pearson's correlation. The common imaging features were "Black turbinate sign" and nonenhancing sino-nasal mucosa (82%), orbital involvement (76%), and diffusion restriction in the optic nerve (24%). Intracranial involvement was seen as perineural extension into the brain (42%), cerebritis (30%), and internal carotid artery involvement (16%).

Conclusions: CA-ROCM is an acute invasive fungal sinusitis with an aggressive clinical course. Black-turbinate sign and peri-antral soft tissue infiltration are early features, whereas extra-nasal tissue infarction, optic nerve diffusion restriction, and vascular invasion are seen with advanced disease.

© 2021 Elsevier Inc. All rights reserved.

Introduction

Mucormycosis is a fulminant opportunistic infection caused by Mucorales, predominantly seen in the immunocompromised population. With the second wave of COVID-19 in India, there has been a dramatic rise in the number of patients with ongoing and prior COVID19 presenting with mucormycosis. A complex interplay between COVID-19 induced immune alterations causing reduced CD4+T and CD8+T cell counts, impaired glycemic control, use of immunosuppressive therapy (ie, corticosteroids), broad-spectrum antibiotics, prolonged hospital stay, oxygen therapy, and ventilatory support has been proposed to be responsible for this super-infection.[1,2]

In the pre-COVID era, the incidence of mucormycosis was much more common in India as compared to the western world.[3] SARS-CoV-2 has further skewed this disease epidemiology. COVID-19 associated rhino-orbital-cerebral Mucormycosis (CA-ROCM) manifests as rapidly progressing invasive fungal sinusitis with high morbidity and mortality. Emergent imaging is vital in confirming the diagnosis, assessing the extent of fungal invasion and associated complications. Our study aimed to analyze the imaging characteristics of CA-ROCM in patients presenting to a tertiary care academic hospital in Rajasthan, India.

Abbreviation: COVID-19, Coronavirus Disease 2019; CA-ROCM, Coronavirus Disease 2019 associated rhino-orbital-cerebral Mucormycosis; SARS-CoV-2, Severe acute respiratory syndrome coronavirus 2; CO-RADS, COVID-19 Reporting and Data System; HbA1c, Glycated haemoglobin; FIESTA-C, Fast Imaging Employing Steady-state Acquisition; CTSI, CT severity score; ENTI, Extra-nasal tissue infarction

*Reprint requests: Dr. Sarbesh Tiwari MD., DM, Department of Diagnostic and Interventional Radiology, All India Institute of Medical Sciences-Jodhpur, Rajasthan 342008.
E-mail address: sarbesh1984@gmail.com (S. Tiwari).

https://doi.org/10.1067/j.cpradiol.2021.09.004
0363-0188/© 2021 Elsevier Inc. All rights reserved.

Material and Methods

Patients

After institutional ethics committee approval, we performed a retrospective review of imaging data of confirmed cases of acute CA-ROCM (confirmed by fungal smears or histopathology) between December 1, 2020 to June 15, 2021. We included all patients with first pre-operative magnetic resonance imaging (MRI) of the brain and paranasal sinus and a history of exposure to COVID-19. Computed tomography (CT) imaging whenever available were also evaluated. Exposure to COVID-19 infection was defined by a positive nasopharyngeal reverse transcription-polymerase chain reaction (RT-PCR) and/ or as those patients with classic chest imaging features of COVID-19 infection, CO-RADS category-5 (COVID-19 Reporting and Data System). Relevant clinical data, treatment regimen, and response were also analyzed. A total of 133 patients with CA-ROCM were enrolled for initial evaluation. Out of 133 patients, 50 patients had pre-operative MR imaging and were included for final analysis. Pre-operative CT scans were available for assessment in 45 of these patients.

Imaging Protocol and Interpretation

All MRI exams were performed on Discovery 750W 3-T (General Electric, Fairfield, USA) using a 24-channel head-neck coil. In addition to conventional MR sequences, short tau inversion recovery (STIR) coronal sequence for orbits, diffusion-weighted imaging (DWI) - propeller for optic nerves, time of flight (TOF) MR angiogram, post-contrast 3DT1 SE & post-contrast FIESTA-C (Fast Imaging Employing Steady-state Acquisition) were acquired in all patients. Contrast-enhanced T1W images were obtained 20-30s after intravenous administration of 0.1-mmol/kg gadobutrol (Gadovist; Bayer Schering Pharma AG, Germany). CT scans for paranasal sinuses were acquired on 256 (128 × 2) slice dual source Somatom Definition Flash (Siemens Healthineers, Germany) using a CT paranasal sinus (PNS) protocol with 120 kV and 100 mA exposure and care dose 4D. All MRI and CT images were evaluated by 2 radiologists in consensus (TY & ST with experience of 11 and 8 years, respectively).

The extent of sinus opacification and signal characteristics of contents were noted for all patients. On MRI, signal intensity (SI) of sinus content were recorded compared with SI of the cerebral cortex. Extra-sinus soft tissue extension seen as an obliteration of normal fat/fat stranding in retroantral region, pterygopalatine fossa, masticator space, and orbit were evaluated. Postcontrast 3D T1 and post contrast FIESTA-C images were used to evaluate perineural spread and intracranial extension (presence or absence of cavernous sinus infiltration, dural enhancement, cerebritis, intracerebral abscess formation, and infarcts). Bone changes (erosions/ destruction) were assessed on CT.

Black turbinate sign, seen in postcontrast T1 sequence was defined as nonenhancement of nasal turbinates and nasal mucosa.[4] Periantral soft tissue infiltration was defined as soft tissue infiltration in retro-antral fat pad along the posterior wall of the maxillary sinus (evaluated on both CT and MR images).[5] Extra-nasal tissue infarction (ENTI) was defined as lack of contrast enhancement in soft tissues on T1 weighted images in and around the sino-nasal tract (evaluated on post contrast T1 images).[6]

Based on the radiological extent, the severity of the disease was classified into 3 stages. Stage I disease was confined only to the nose and paranasal sinuses. Stage II disease included extension into orbits, hard palate, and oral cavity (sites which were surgically resectable with minimal morbidity).[7,8,9] Intracranial extension was considered stage III disease.

Statistical Analysis

Statistical analysis was done using the Statistical Package for Social Sciences (SPSS) version 23.0 (Armonk, NY: IBM Corp). Qualitative variables like age, gender, comorbidities, clinical symptoms, and imaging features were described by frequency and percentages. Pearson correlation test was used for determining the degree of association between disease stage and diabetes, HbA1c levels, steroid intake, use of oxygen therapy, and CTSI. Results with P-value <0.05 were regarded as statistically significant.

Results

Out of 50 patients, 31 patients were male (62%). The mean age was 49.5 years (range 28 − 70 years). The mean CT severity score (CTSI) was 9.8 ± 6.25 (available in 42 patients). A prior history of hospitalization was present in 22 patients (44%), history of steroid intake and oxygen supplementation was present in 22 patients (44%) and 19 patients (38%) respectively. The mean time since diagnosis of COVID-19 and imaging for CA-ROCM was 14.2 +/-7.12 days.

Twenty patients were previously diagnosed with type 2 diabetes (DM), 16 of them had poorly controlled glycemic index (elevated HbA1c > 6.5 or random blood sugar levels> 200 mg/dl). Twenty-three patients were newly diagnosed with diabetes at current presentation (based on elevated HbA1 c levels of > 6.4%). Of the remaining 7 patients, 5 were prediabetic (HbA1c glycemic indices between 6% and 6.4%). Only 2 patients had normal glycemic control and one of them was immunocompromised due to a previous renal transplant.

Significant positive correlation between HbA1c level and disease stage (r = .443, p-value = 0.005, n = 39) was present. Mean HbA1c in stage 1, stage 2, and stage 3 were 8.8 ± 2.27, 8.8 ± 2.18, and 11.3 ± 2.44 respectively (Table 1). The correlation of the disease stage with a history of steroid intake (P-value = 0.417), oxygen supplementation (P-value = 0.949), and the CTSI ((P-value = 0.716) was not statistically significant (Table 2).

The study cohort had 7 patients in stage I disease with isolated sino-nasal involvement (Fig 1), 18 patients in stage II disease (Fig 2) with sino-nasal-orbital involvement, and 25 patients in stage III disease with intracranial involvement (Fig 3). The ethmoid and maxillary sinuses were the most frequently involved in 46 (92%) patients followed by sphenoid 41 (82%), and frontal sinuses 28 (56%).

Sinus hyperdensity was seen in 32 patients (64%). Bone erosion or destruction was present in 42 patients (84%). The commonest site of bone erosion/destruction was maxilla in 20 patients (40%), followed by lamina papyracea in 6 patients (12%). Black turbinate sign and non-enhancing sino-nasal mucosa (Fig 4) were observed in 41 patients (82%). Peri antral soft tissue infiltration was seen in 37 patients (74%).

The orbital extension was present in 38 patients (76%) which included all stage II and 20 stage III patients. Proptosis was present in 27 patients (54%) more commonly seen on the right side (18/27 cases). Extraocular muscle involvement was seen in all patients with orbital involvement with inferior rectus being most commonly involved muscle in 20 (40%), followed by medial rectus in 18 (36%).

TABLE 1
Risk factors for Coronavirus disease-2019 associated Rhino-Orbito-Cerebral Mucormycosis (CA-ROCM)

Stage of the disease	Age (Years)	Male/ Female	Diabetes & Prediabetes	HbA1c	Steroid Use	CTSI(average)
Stage I (n = 7)	47.5 ± 15.04	5/2	6 (85.7%)	8.8 ± 2.27	2 (28.5%)	11.8 ± 6.61
Stage II (n = 18)	54.2 ±11.97	12/6	17 (94.4%)	8.8 ± 2.18	8 (44.4%)	8.75 ± 6.57
Stage III (n = 25)	46.6 ± 11.06	14/11	25 (100%)	11.3 ± 2.44	12 (48%)	10.0 ± 5.97

TABLE 2
Correlation between stage of disease and various patient parameters

		Diabetes	HbA1c Level	Steroid use	Oxygen supplementation	CTSI
Stage of the disease	Pearson Correlation	0.366	0.443	0.117	0.009	-0.58
	P-value	0.009	0.005	0.417	0.949	0.716

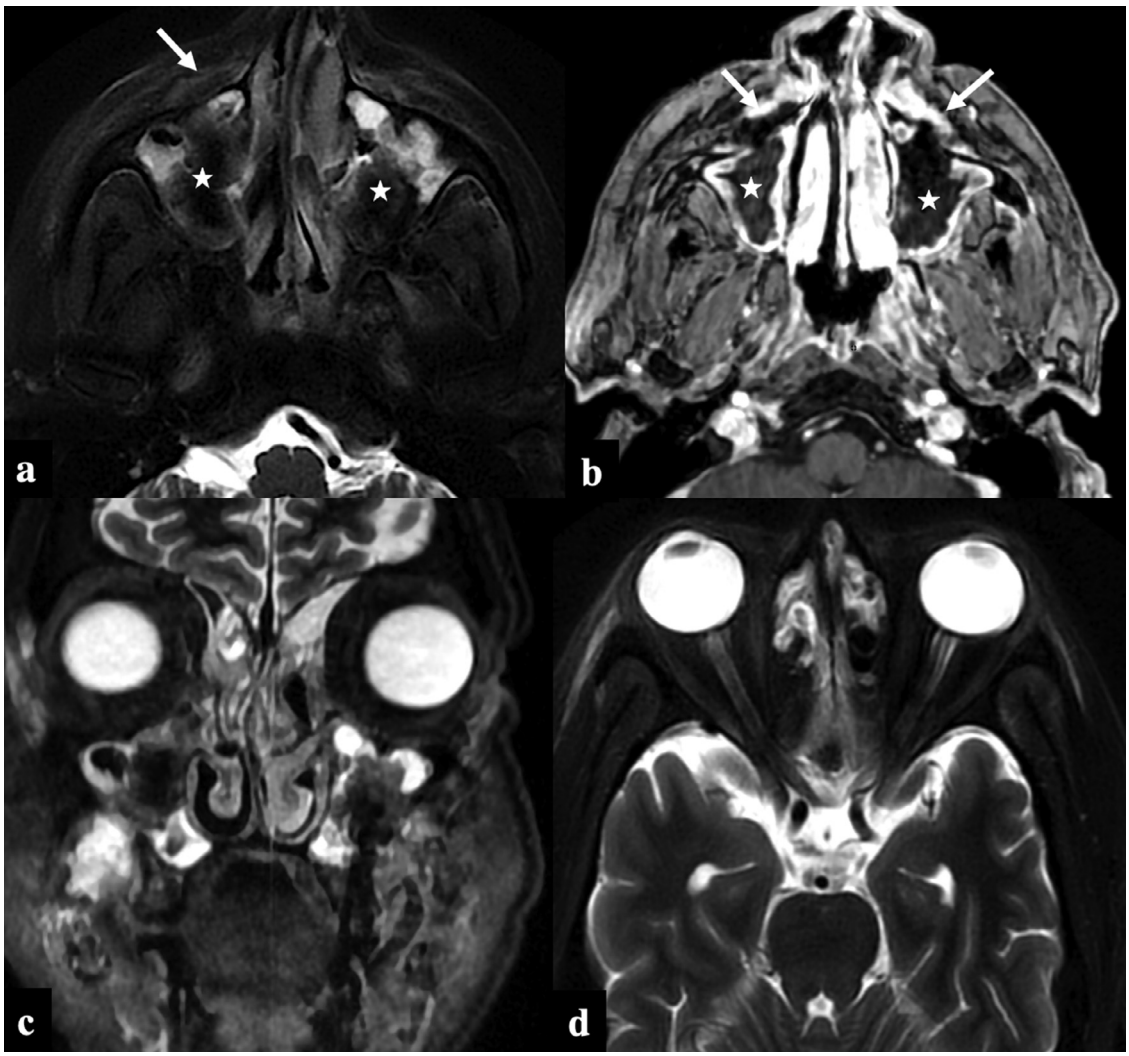

FIG 1. COVID-19 associated Rhino-Orbital-Cerebral Mucormycosis, Stage I disease. A 40-year-old male recovering from COVID-19 infection (23 days post covid status), presented with facial pain. Axial T2FS (A) and post-contrast 3D T1 GRE (B) images show T2 hypointense soft tissue (asterix) within bilateral maxillary sinuses with infiltration of the bilateral anterior periantral fat planes (arrows). Absence of orbital and brain involvement on the coronal STIR (C) and axial T2FS (D) images.

Orbital apex involvement was seen in 23 (46%) patients. Diffusion restriction of the optic nerve was seen in 12 (24%) patients. Conical deformation of the posterior aspect of the ocular globe due to markedly raised intra-orbital pressure ("guitar-pick" sign) was observed in 6 (12%) patients (Fig 5).

Lack of enhancement of the peri-sinus soft tissues defined as extra-nasal tissue infarction was demonstrated in 29 (58%) cases (Fig 6). The pterygopalatine fossa was the most common site of peri-sinus extension noted in 34 (68%) patients followed by infratemporal fossa 33 (66%).

Cavernous sinus was involved in 16 patients (32 %) with isolated right-sided involvement in 8 cases and bilateral in 4 cases. Thickening and enhancement of dura was the most frequent intracranial abnormality reported in 19 (38%) patients followed by cerebritis due to brain parenchymal invasion in 15 (30%) patients. Cerebral ischemic infarcts secondary to the vascular invasion were less common, seen in 8 (16%) cases.

Perineural extension of infection was noted in 21 (42%) patients with involvement of multiple cranial nerves in few patients. Most commonly, the perineural spread was present along the trigeminal nerve and its branches in 16 (32%) patients (Fig 7), followed by olfactory and facial nerves in 2 patients each.

Analysis of MR angiographic images showed occlusion of the third part of the internal maxillary artery (pterygopalatine segment) in 14 patients (28%). Thrombosis of the ophthalmic artery was seen in 7 patients (14%) with all patients having orbital apex involvement. Narrowing and irregularity of the internal carotid artery were seen in 8 patients (16%)(Fig 8). None of our patients had any mycotic aneurysms detected on imaging (Table 3).

Discussion

Rhino-orbital-cerebral mucormycosis is invasive fungal sinusitis having an acute or chronic course.[10] Chronic ROCM (with a clinical

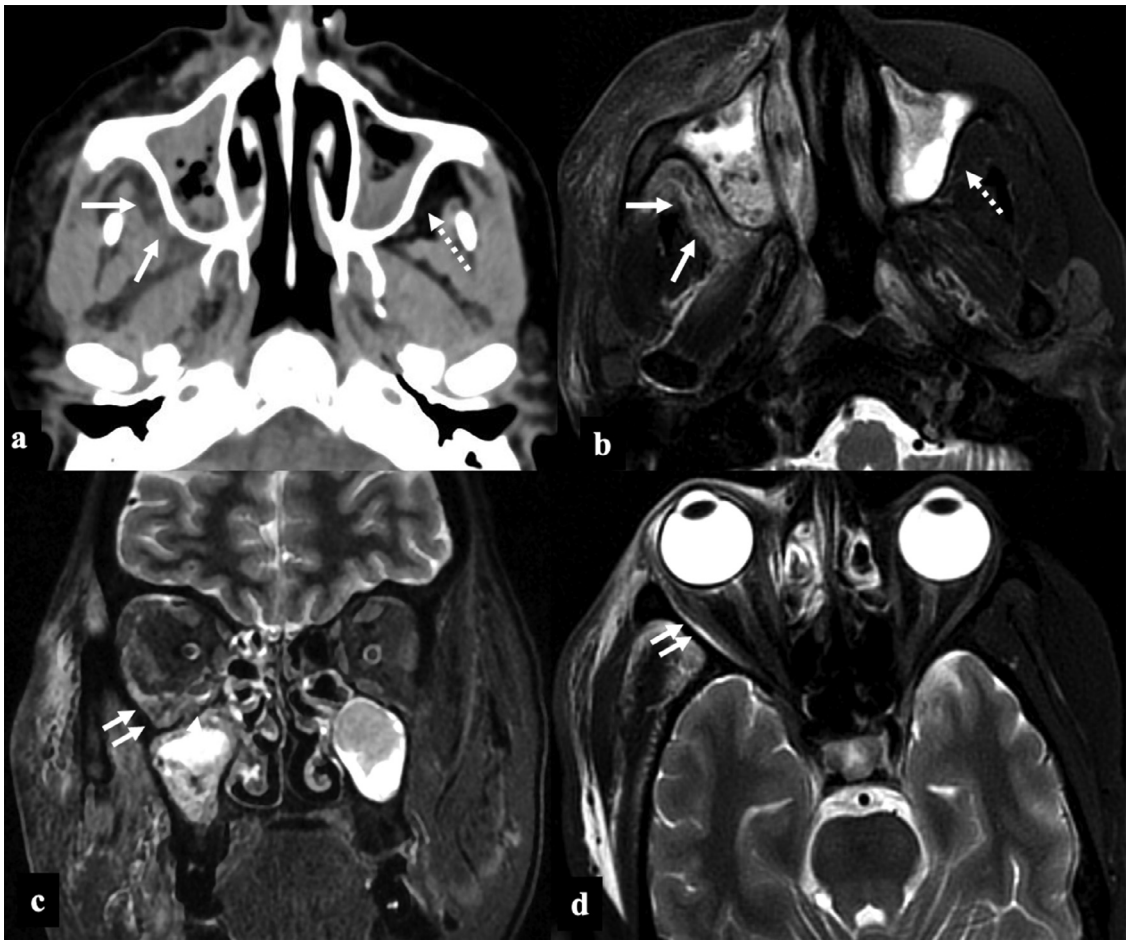

FIG 2. COVID-19 associated Rhino-Orbital-Cerebral Mucormycosis, Stage II disease. A 56-year-old diabetic lady, on treatment for COVID-19 infection (10th day) with intravenous steroids and high flow nasal oxygen therapy, presented with facial pain, swelling and bluish discoloration of skin. Paranasal sinus axial NCCT (A) and axial T2FS (B) images at the level of maxillary sinuses show posterior periantral soft tissue infiltration (arrows) suggestive of peri-sinus extension of disease. Retro-maxillary fat pad is normal on the left side (dashed arrows). Coronal STIR (C) and axial T2FS (D) images at the level of orbits show extra-conal soft tissue infiltrates involving the inferior and lateral compartment of the right orbit (double arrows).

course of more than 4 weeks) can be chronic invasive fungal sinusitis and chronic granulomatous invasive fungal sinusitis. COVID-19 associated rhino-orbital-cerebral mucormycosis (CA-ROCM) usually manifests as an acute fulminant invasive form during the active or convalescent phase of COVID-19 disease and has a high mortality (as high as 49%).[11]

Mucormycosis primarily affects immunocompromised patients with only 9%-19% cases documented in immunocompetent individuals.[12] In our study, elevated HbA1c indicative of poor glycemic control positively correlated with increased invasiveness and aggressive fungal disease. Previous history of steroids, hospital stay, oxygen supplementation, and chest CT severity score were also recorded in patients with severe mucor infection but could not achieve statistical significance.

Mucor is a universal saprophytic fungus found in soil and vegetation. Inhalation is the primary route of inoculation, where the fungus colonizes the paranasal sinuses and subsequently spreads via direct soft-tissue and bone invasion, perivascular, or perineural routes to orbit and brain.[9] Intracranial spread can occur by erosion of lamina papyracea, cribriform plate, along cranial nerves, and along the branches of ethmoidal, ophthalmic, internal carotid, and basilar artery.[9,12,13] We found the ethmoid and maxillary sinuses to be the more often involved sinus followed by sphenoid and frontal sinuses. Further, the majority of our patients had orbital (stage II) and intracranial disease (stage III) at presentation suggesting an aggressive clinical course and invasive nature of CA-ROCM.

Sino-nasal disease is identified on imaging by opacification of paranasal sinuses with high attenuation content, nodular mucosal thickening, and absence of fluid level. The sinus content invariably appears hypointense on T2 images secondary to the presence of iron and manganese in the fungal elements (Fig 1).[14,15] "Black turbinate Sign" identified as persistent nonenhancement of the nasal turbinates on postcontrast sequences is an early MRI feature of nasal mucormycosis.[4,16] Similarly nonenhancement of nasal and sinonasal mucosa is also described and both of these signs represent devitalized and necrotic tissue secondary to microvascular invasion (Fig 4). Periantral fat infiltration is also an early imaging feature suggestive of infiltration into fat outside maxillary sinus secondary to bone erosion or spread via perivascular channels[5] (Fig 2A & 2B).

Extension of fungal disease to pterygopalatine fossa may occur either through direct erosion of sinus wall or perivascular or perineural spread. Involvement of pterygopalatine fossa forms a route of entry of infection into the middle cranial fossa and cavernous sinus.[17] We observed these features in over two-thirds of cases that were associated with either stage II or stage III disease.

Proptosis is a common feature in patients with CA- ROCM suggesting orbital invasion and raised intra-orbital pressure resulting from inflammatory changes in retro-orbital fat and orbital apex. Muscle thickening and abnormal enhancement with lateral displacement of medial and inferior rectus muscles occur by contiguous spread

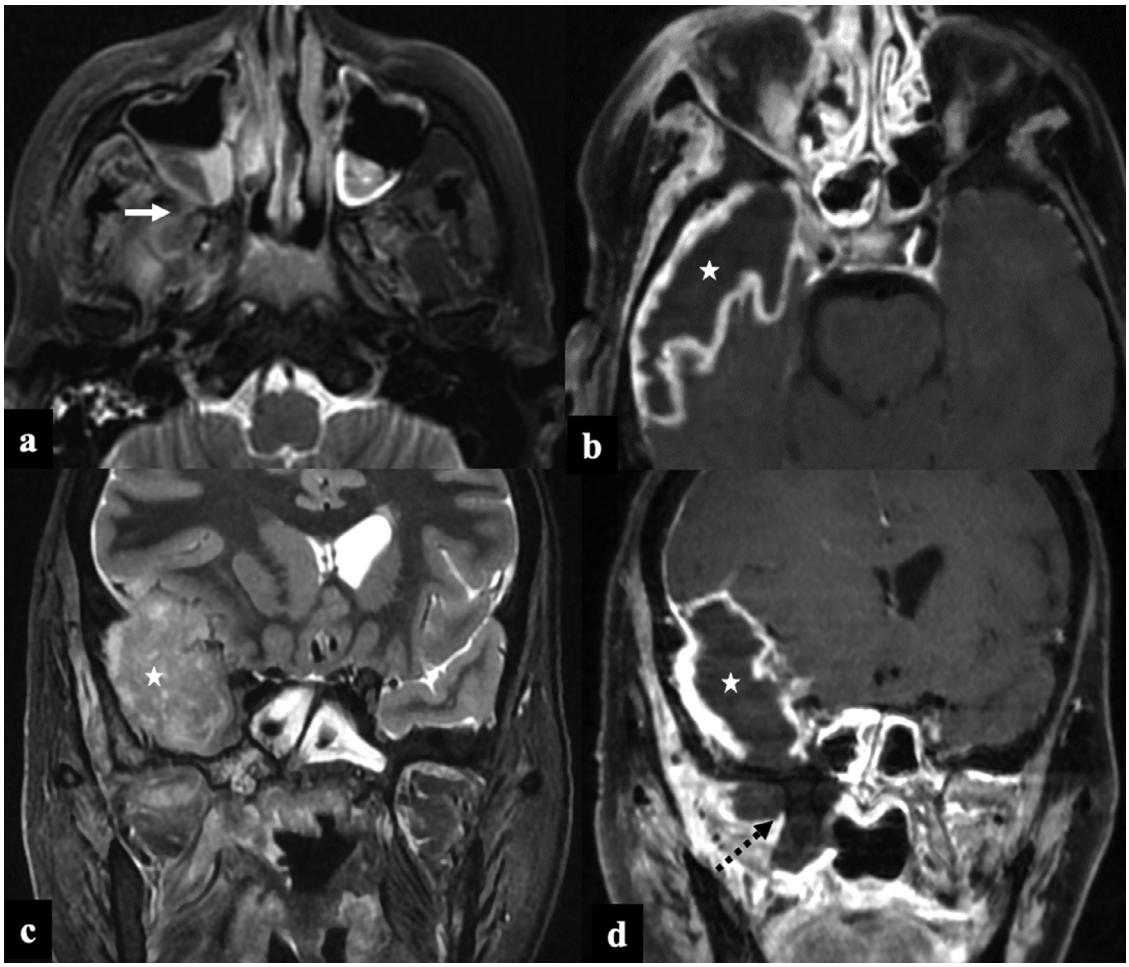

FIG 3. COVID-19 associated Rhino-Orbital-Cerebral Mucormycosis, Stage III disease. A 35-year-old female, post covid-19 status (30th day), presented with headache and right facial swelling. Axial T2FS image (A) shows hypointense soft tissue within the right maxillary sinus with infiltration of posterior periantral fat and pterygoid muscles (arrow). Post-contrast 3D T1 cube (B, D) and coronal STIR (C) images show thick walled peripherally enhancing abscess along the right temporal lobe (asterix). Also note the non enhancing infarcted soft tissue adjoining right pterygoid plates (black dashed arrow) contiguously extending into temporal lobe.

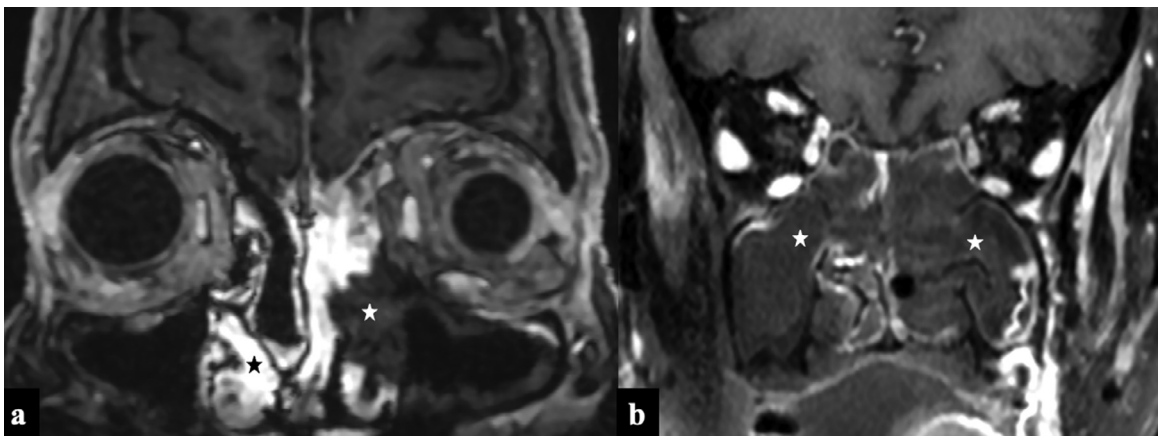

FIG 4. Black Turbinate sign in 2 patients on coronal postcontrast T1W images with rhino-orbital-cerebral mucormycosis. (A) Image showing "black turbinate sign" with non-enhancing left middle and part of inferior turbinate (white asterix) and non-enhancing left maxillary sinus mucosa. Note the normal enhancing nasal turbinates on the right side (black asterix). (B) Image showing bilateral non enhancing nasal turbinates and nasal mucosa (bilateral "black-turbinate" & "black-mucosa" sign).

from ethmoidal and maxillary sinuses respectively.[14] Furthermore, perineural spread also accounts for the orbital spread of disease.

Diffusion restriction of the optic nerve can be secondary to the invasion of the ophthalmic artery at the orbital apex or the optic canal. It is an ominous sign and is a predictor of irreversible vision loss. [18] Diffusion restriction of the optic nerve was better demonstrated on the propeller-based diffusion weighted images acquired with 3 mm thickness (5c & 5d). This sequence may be an add-on in a patient with orbital apex disease. "Guitar-Pick" sign (Fig 5A & 5B) which is a conical deformation of the posterior aspect of the ocular globe is seen due to severely raised intra-orbital pressure (orbital compartmental syndrome).

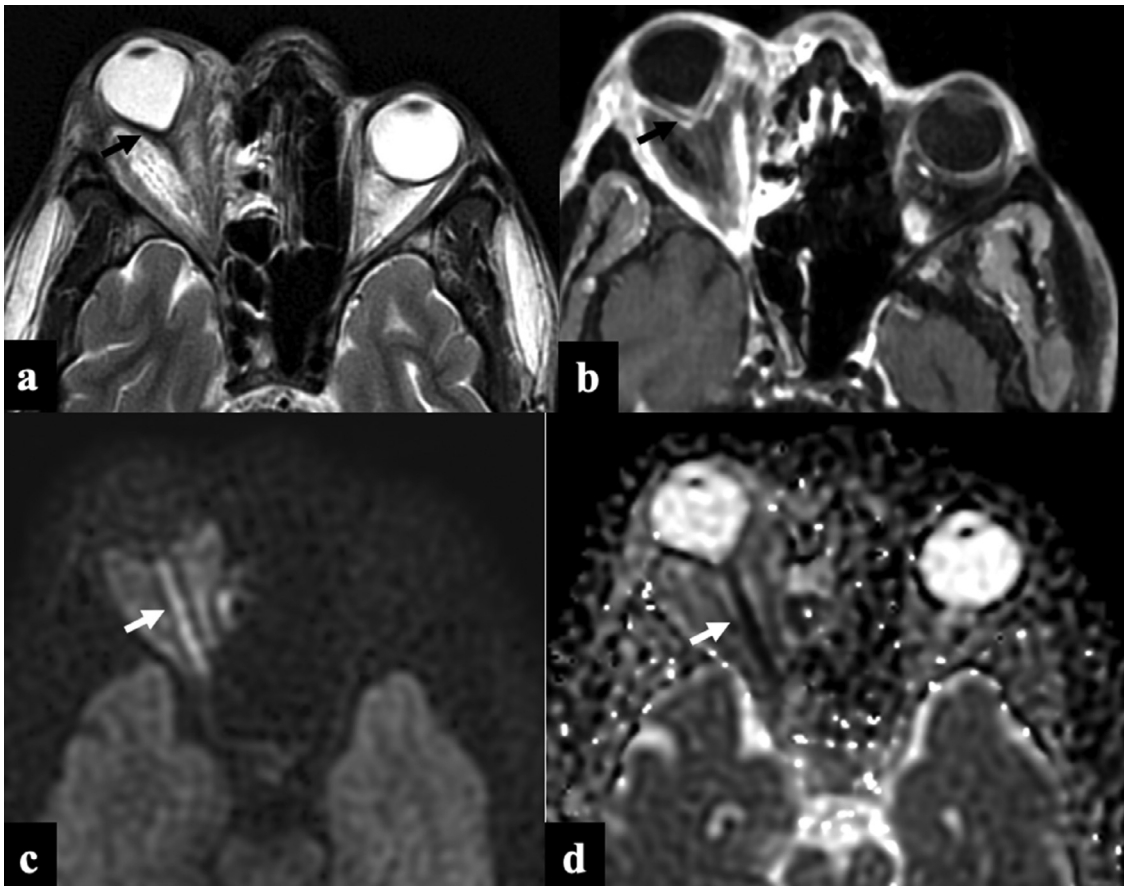

FIG 5. Guitar Pick Sign. Axial T2W (A) and postcontrast T1W (B) images showing the conical deformation of right posterior globe (black arrow) resulting in "guitar pick sign" with non enhancing infarcted tissue in the retro-orbital fat. Note the diffusion restriction of the right optic nerve (white arrow) on the DWI propeller image (C) and ADC (D) map.

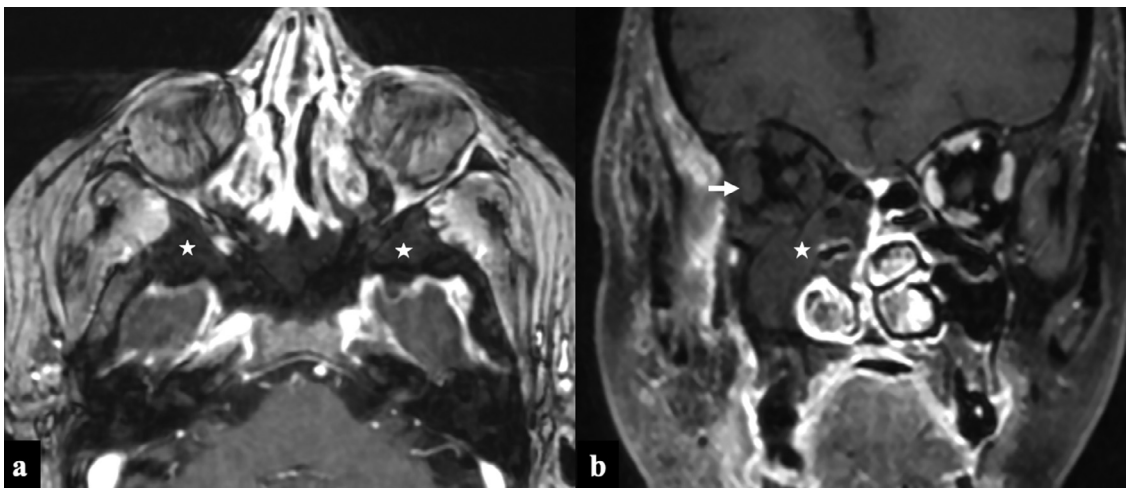

FIG 6. Extra-nasal tissue infarction in 2 patients with COVID-19 associated Rhino-Orbital-Cerebral Mucormycosis. Axial postcontrast 3D T1 GRE image (A) showing absence of enhancement of bilateral greater wings and body of sphenoid (asterix), adjoining clivus, adjacent soft tissues suggestive of infarction. Coronal post-contrast 3D T1W image (B) displaying non enhancement of right middle turbinate, mucosa of right maxillary and ethmoid sinuses (asterix). Note the non-enhancement of the right extra-ocular muscles suggestive of tissue infarction.

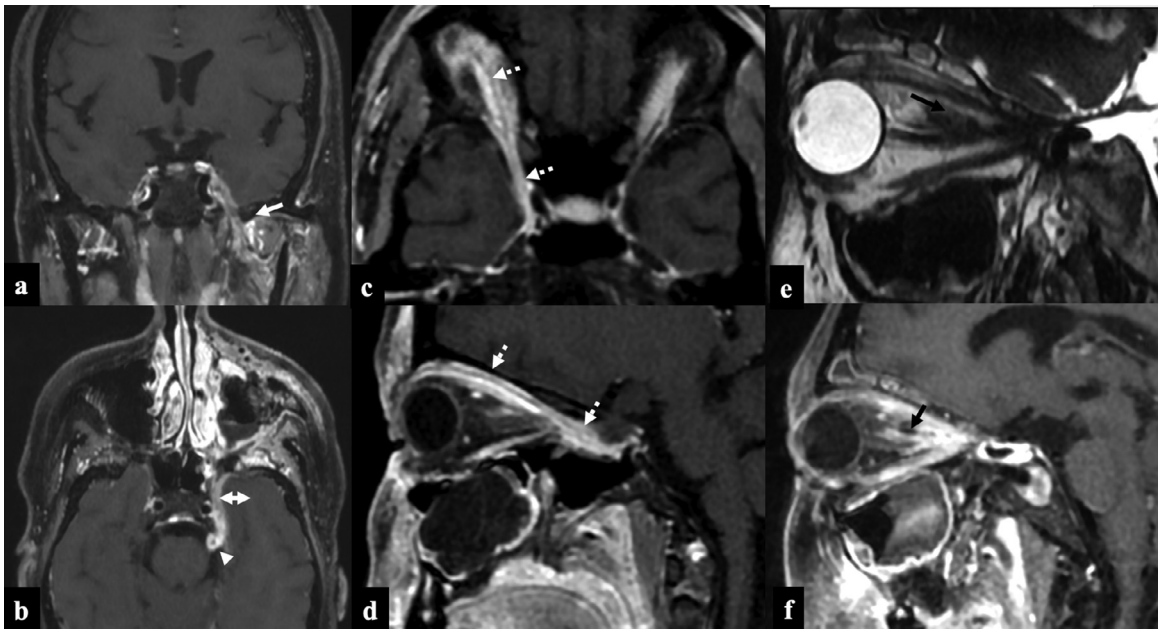

FIG 7. Patterns of perineural spread in 3 patients with COVID-19 associated Rhino-Orbital-Cerebral Mucormycosis. Patient 1: Post-contrast T1W coronal (A), axial (B) images demonstrate thickened and enhancing left mandibular nerve (arrow), left maxillary nerve (double headed arrow) and left trigeminal nerve (arrowhead). Patient 2: Postcontrast T1W axial (A), sagittal (B) images show thickening and enhancement of ophthalmic division (V1, dashed arrows) of right trigeminal nerve. Patient 3: Sagittal T2W image (E) shows hypointense nodular thickening along the optic nerve sheath which shows enhancement on sagittal post-contrast T1W image (F).

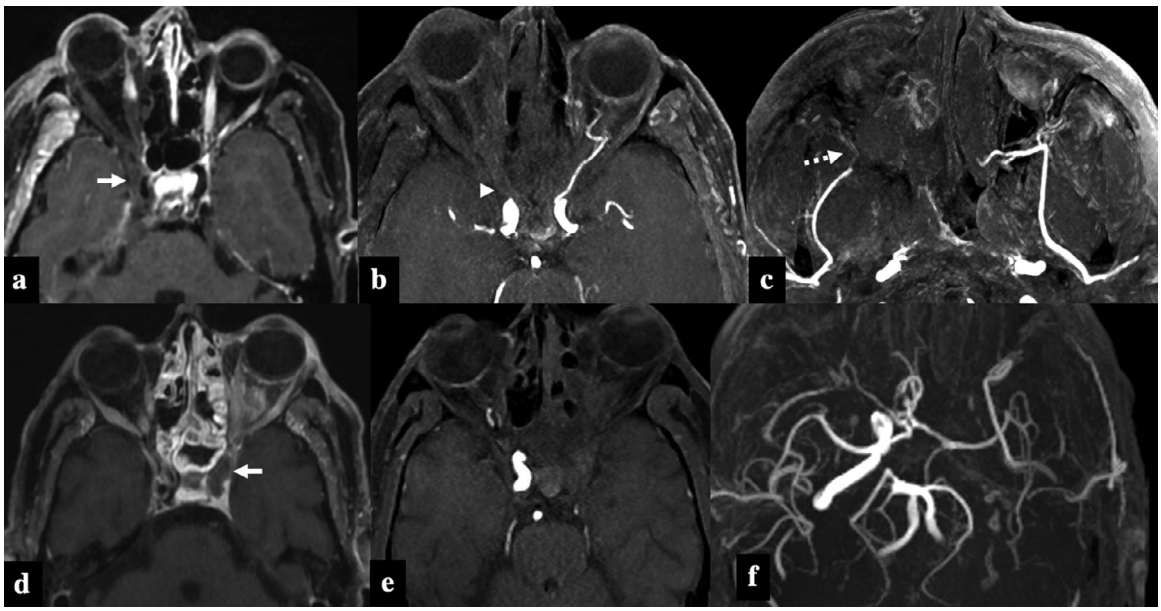

FIG 8. Patterns of vascular invasion in 2 patients with COVID-19 associated Rhino-Orbital-Cerebral Mucormycosis. Patient 1: Postcontrast axial T1FS image (A) shows right-sided proptosis with non enhancement of right sclera and extra-ocular muscles suggesting extra-nasal tissue infarction. Soft tissue infiltration of the right orbital apex and right cavernous sinus is evident (white arrow) with narrowing of right ICA flow void. Axial 3D-TOF MR angiography MIP images show absence of flow related enhancement in right ophthalmic artery (B, arrow-head) and third segment of right internal maxillary artery (C, dashed arrow). Patient 2: Post-contrast axial T1FS image (D) shows left-sided proptosis with enhancing soft tissue in retro-orbital fat, infiltration of ipsilateral cavernous sinus and cavernous segment of ICA (arrow). Axial 3D-TOF MR angiography MIP images (E & F) show absence of flow related signal in left ICA.

Extra-nasal tissue infarction (ENTI) is defined as a lack of contrast enhancement on T1 weighted images in the surrounding tissues

TABLE 3
Imaging characteristics for Coronavirus disease-2019 associated Rhino-orbito-cerebral Mucormycosis (CA-ROCM)

Imaging Features	Number (out of 50) (Percentage)
Black Turbinate sign/Non enhancing sino-nasal mucosa	41 (82%)
Peri-antral soft tissue inflammation	37(74%)
Extra-ocular muscle involvement	38(76%)
Orbital apex	23(46%)
Diffusion restriction of optic nerve	12(24%)
Extra-nasal tissue infarction	29(58%)
Pterygopalatine fossa	34(68%)
Infratemporal fossa	33(66%)
Cavernous sinus	16(32%)
Pachymeningeal involvement	19(38%)
Cerebritis/early abscess formation	15(30%)
Cerebral ischemic Infarct	8(16%)
Perineural Extension	21(42%)
Vascular invasion of ICA	8(16%)

Abbreviation: ICA-Internal carotid artery.

outside the sino-nasal tract.[6] It serves as a surrogate for the black-turbinate sign in extra nasal tissue (Fig 6). This is due to infarction of sinus and peri-sinus tissue secondary to vascular invasion and necrosis caused by the fungus. In 8 patients with ENTI involving the maxilla, we observed air within the maxillary alveolus (Fig 9A). This might be secondary to microscopic extension of air from the sinus into the maxillary alveolus or secondary to osteonecrosis. These patients more commonly presented at the dental clinics with symptoms of loosening of teeth, dental pain and discomfort.

Pachymeningeal thickening and enhancement were the most common features of intracranial involvement in our study, followed by cavernous sinus invasion and cerebritis secondary to brain invasion. Basifrontal and anteromedial temporal regions were common sites of cerebritis and fungal abscess formation (Fig 3). Perineural spread is a very important pathway of disease progression with the maxillary division (V2) and ophthalmic division (V1) of trigeminal nerve being the most common nerves involved. (Fig 7). Further, we also observed that the anteromedial temporal region fungal abscesses were associated with contiguous inflamed and thickened maxillary division, which might represent the cause for such abscess formation.

The pathobiology of mucormycosis is characterized by the proliferation of angio-invasive hyphae within the elastic lamina of large to intermediate sized arteries[19] which necessitates a meticulous evaluation of intracranial and facial vasculature (Fig 10). Ophthalmic, internal carotid and pterygopalatine segments of internal maxillary artery are common arteries affected by invasive fungal disease extending into the orbital apex, cavernous sinus, and pterygomaxillary fissure respectively (Fig 8).[8] Therefore, it is prudent to perform angiographic sequences in the evaluation of patients with invasive fungal disease.

Our cohort did not have any patient with complete occlusion of ICA or pseudoaneurysm formation from the cavernous segment of ICA which has been reported previously with subacute or chronic mucormycosis. This might be explained by short duration of illness in all patients presenting with CA-ROCM. The main limitation of our study is that it is a single center retrospective study, though patients are referred from nearby geographic regions. Intermediate and long term follow up in survivors needs to be assessed to study the differences in natural history attributable to COVID19 coinfection.

Conclusion

COVID-19 associated rhino-orbital-cerebral mucormycosis is an acute invasive fungal sinusitis with an aggressive clinical course. Patients with poor glycemic control are more prone to develop more severe infection. Comprehensive imaging evaluation is vital to determine extent of involvement and complications to guide surgery. Black-turbinate sign and periantral soft tissue infiltration are seen in early stage of infection. Extra-nasal tissue infarction, optic nerve diffusion restriction, and vascular invasion are features seen in more severe disease.

Declaration of Competing Interest

None

FIG 9. Patterns of bone involvement in 2 patients with COVID-19 associated Rhino-Orbital-Cerebral Mucormycosis. Patient 1: Presented with loosening of maxillary teeth and dental pain. Coronal image (A) shows multiple air foci in right sided maxillary alveolus (dashed arrow). Patient 2: Axial image (B) shows extensive osteolytic changes in right maxilla and zygomatic bone with associated soft tissue.

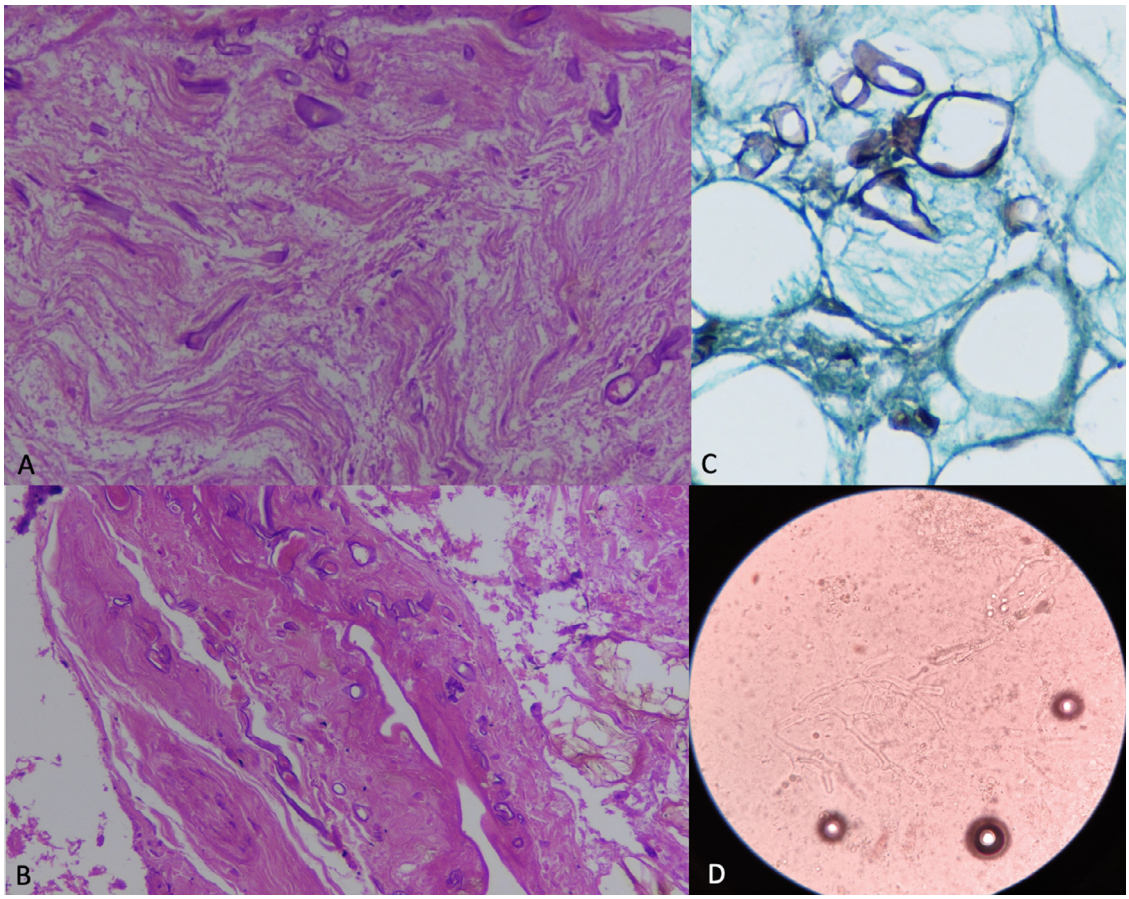

FIG 10. Microscopic examination of an orbital exenteration specimen (A,B) Hematoxylin-eosin (H&E) sections at higher magnification (400x), (A) Longitudinal section of a nerve in the retro-orbital fat with few broad, ribbon-like irregular hyphae consistent with Mucor. (B) Wall of blood vessel is invaded by broad irregular fungal hyphae of Mucor confirming angioinvasion. (C) Gomori Methenamine Silver (GMS) (400x) stain highlighting the fungal hyphae. (D) KOH mount (400x) showing broad hyaline pauciseptate hyphae with right angled branching suggestive of mucormycosis.

Financial Disclosure

None

References

1. Rawson TM, Moore LS, Zhu N, et al. Bacterial and fungal coinfection in individuals with coronavirus: A rapid review to support COVID-19 antimicrobial prescribing. Clinical Infectious Diseases 2020;71:2459–68.
2. Sharma S, Grover M, Bhargava S, et al. Post coronavirus disease mucormycosis: a deadly addition to the pandemic spectrum. The Journal of Laryngology & Otology 2021:1–6.
3. Skiada A, Pavleas I, Drogari-Apiranthitou M. Epidemiology and diagnosis of mucormycosis: An update. Journal of Fungi 2020;6:265.
4. Safder S, Carpenter JS, Roberts TD, et al. The "black turbinate" sign: An early MR imaging finding of nasal mucormycosis. Am j neuroradiol 2010;31:771–4.
5. Silverman CS, Mancuso AA. Periantral soft-tissue infiltration and its relevance to the early detection of invasive fungal sinusitis: CT and MR findings. American journal of neuroradiology 1998;19:321–5.
6. Seo J, Kim HJ, Chung SK, et al. Cervicofacial tissue infarction in patients with acute invasive fungal sinusitis: Prevalence and characteristic MR imaging findings. Neuroradiology 2013;55:467–73.
7. Rupa V, Maheswaran S, Ebenezer J, et al. Current therapeutic protocols for chronic granulomatous fungal sinusitis. Rhinology 2015;53:181–6.
8. Mazzai L, Anglani M, Giraudo C, et al. Imaging features of rhinocerebral mucormycosis: From onset to vascular complications. Acta Radiologica 2021:0284185120988828.
9. Therakathu J, Prabhu S, Irodi A, Sudhakar SV, Yadav VK, Rupa V. Imaging features of rhinocerebral mucormycosis: A study of 43 patients. The Egyptian J Radiol and Nuclear Medicine 2018;49:447–52.
10. deShazo RD, O'Brien M, Chapin K, et al. A new classification and diagnostic criteria for invasive fungal sinusitis. Archives of Otolaryngol–Head & Neck Surg 1997;123:1181–8.
11. John TM, Jacob CN, Kontoyiannis DP. When Uncontrolled Diabetes Mellitus and Severe COVID-19 Converge: The perfect storm for mucormycosis. J of Fungi 2021;7:298.
12. Adulkar NG, Radhakrishnan S, Vidhya N, et al. Invasive sino-orbital fungal infections in immunocompetent patients: A clinico-pathological study. Eye 2019;33:988–94.
13. Palacios E, Rojas R, Rodulfa J, et al. Magnetic resonance imaging in fungal infections of the brain. Topics in Magnetic Resonance Imaging 2014;23:199–212.
14. Chan LL, Singh S, Jones D, et al. Imaging of mucormycosis skull base osteomyelitis. Am j neuroradiol 2000;21:828–31.
15. Mossa-Basha M, Ilica AT, Maluf F, et al. The many faces of fungal disease of the paranasal sinuses: CT and MRI findings. Diagnostic and Interventional Radiol 2013;19:195.
16. Han Q, Escott EJ. The black turbinate sign, a potential diagnostic pitfall: Evaluation of the normal enhancement patterns of the nasal turbinates. Am J Neuroradiol 2019;40:855–61.
17. Mathur S, Karimi A, Mafee MF. Acute optic nerve infarction demonstrated by diffusion-weighted imaging in a case of rhinocerebral mucormycosis. American journal of neuroradiology 2007;28:489–90.
18. Theoret J, Sanz GE, Matero D, et al. The "guitar pick" sign: A novel sign of retrobulbar hemorrhage. Canadian Journal of Emergency Medicine 2011;13:162–4.
19. Turgut M, Challa S, Akhaddar A. Fungal Infections of the Central Nervous System: Pathogens, Diagnosis, and Management. editors Springer; 2019.